Regulation of inflorescence architecture by intertissue layer ligand–receptor communication between endodermis and phloem

Naoyuki Uchida[a,1], Jin Suk Lee[b,1], Robin J. Horst[b], Hung-Hsueh Lai[b], Ryoko Kajita[c], Tatsuo Kakimoto[c], Masao Tasaka[a], and Keiko U. Torii[b,d,e,2]

[a]Graduate School of Biological Sciences, Nara Institute of Science and Technology, Nara 630-0192, Japan; [b]Department of Biology, University of Washington, Seattle, WA 98195; [c]Department of Biological Science, Graduate School of Sciences, Osaka University, Osaka 565-0871, Japan; [d]Howard Hughes Medical Institute, University of Washington, Seattle, WA 98195; and [e]Precursory Research for Embryonic Science and Technology, Japan Science and Technology Agency, Tokyo 102-0075, Japan

Edited by Mark Estelle, University of California at San Diego, La Jolla, CA, and approved March 1, 2012 (received for review October 29, 2011)

Multicellular organisms achieve final body shape and size by coordinating cell proliferation, expansion, and differentiation. Loss of function in the *Arabidopsis ERECTA* (*ER*) receptor-kinase gene confers characteristic compact inflorescence architecture, but its underlying signaling pathways remain unknown. Here we report that the expression of *ER* in the phloem is sufficient to rescue compact *er* inflorescences. We further identified two *EPIDERMAL PATTERNING FACTOR-LIKE* (*EPFL*) secreted peptide genes, *EPFL4* and *EPFL6/CHALLAH* (*CHAL*), as redundant, upstream components of *ER*-mediated inflorescence growth. The expression of *EPFL4* or *EPFL6* in the endodermis, a layer adjacent to phloem, is sufficient to rescue the *er*-like inflorescence of *epfl4 epfl6* plants. EPFL4 and EPFL6 physically associate with ER in planta. Finally, transcriptome analysis of *er* and *epfl4 epfl6* revealed a potential downstream component as well as a role for plant hormones in EPFL4/6- and ER-mediated inflorescence growth. Our results suggest that inter-cell layer communication between the endodermis and phloem mediated by peptide ligands and a receptor kinase coordinates proper inflorescence architecture in *Arabidopsis*.

peptide signal | pedicel elongation | cell–cell communication

Organ morphogenesis in multicellular organisms relies on coordinated cell proliferation and differentiation of diverse cell types, each with specific functions. In higher plants, aboveground organs are generated via continual activity of the shoot apical meristem (SAM). Because plant cells do not migrate during organogenesis, cell–cell communication within and between tissue layers is critical for elaboration of organ shape.

Inflorescence stems, which dominate the overall architecture of the model plant *Arabidopsis thaliana*, are initially formed from the rib zone of the SAM and are composed of radially patterned tissue layers of epidermis, cortex, endodermis, vasculature, and pith. Each tissue layer has specific functions; the epidermis serves as an interface between the plant and the external environment (1), the stem endodermis plays a role in shoot gravitropic response (2), and the vasculature contains the essential conductive tissues phloem and xylem (3). How these distinct tissue layers coordinate their growth and development to organize inflorescence architecture has not yet been fully explored.

The *Arabidopsis ERECTA* (*ER*) gene promotes inflorescence elongation. *er* plants exhibit a characteristic compact inflorescence with short internodes and short pedicels (4). *ER* encodes a receptor-like kinase (RLK) with an extracellular leucine-rich repeat (LRR) domain, suggesting that it acts as a signaling receptor (5). Along with inflorescence development, *ER* regulates multiple developmental processes as well as environmental and biotic responses (6). Among these, the role of *ER* in stomatal patterning has been well studied. ER and its two closely related RLKs, ER-LIKE1 (ERL1) and ER-LIKE2 (ERL2), inhibit stomatal differentiation and enforce proper stomatal spacing (7). These receptors perceive signaling ligands, EPF1 and EPF2, which are secreted from neighboring stomatal precursors (7–10, 22). An LRR receptor-like protein, TOO MANY MOUTHS (TMM), modulates stomatal patterning, by associating with ER-family RLKs (7, 11, 22). EPFL9/Stomagen and EPFL6/CHAL influence stomatal patterning through internal tissue layers (12–14). In contrast to stomatal development, the underlying mechanism of ER-mediated inflorescence development remains unclear.

Here we report that proper inflorescence architecture in *Arabidopsis* can be specified by intertissue layer communication between the phloem and the endodermis mediated by ER and its signaling ligands, EPFL4 and EPFL6, 2 of the 11 members of the EPFL family of secreted cysteine-rich peptides (CRPs) (9, 14, 15). The endodermal expression of *EPFL4* or *EPFL6* and the phloem expression of *ER* are sufficient for proper inflorescence growth. Consistent with our genetic study, in vivo binding assays demonstrate that EPFL4 and EPFL6 biochemically associate with ER. Finally, transcriptome analysis implicates the plant hormones auxin and gibberellin (GA) as potential factors promoting non–cell-autonomous growth of the inflorescence via EPFL4/6 and ER.

Results

Phloem-Specific Expression of *ER* Is Sufficient for Proper Inflorescence Architecture. To understand the mechanism of *ER*-mediated inflorescence growth, we first examined the expression of *ER* in inflorescence stems at high resolution. As reported previously (16, 17), a reporter β-glucuronidase (GUS) analysis showed that *ER* promoter is highly active in growing inflorescence stems and pedicels (Fig. 1*A*). Thin tissue sectioning further delineated high *ER* promoter activity in the epidermis, phloem, and xylem (Fig. 1*B*).

To determine whether *ER* expression in a specific tissue layer is sufficient to drive *ER*-mediated inflorescence growth, we next uncoupled the *ER* expression in epidermis, phloem, and xylem tissues. For this purpose, tissue-specific rescue experiments were performed by expressing an epitope-tagged *ER* (*ER-FLAG*) in *er* mutant under the control of well-studied tissue-specific promoters: *AtSUC2* for phloem (18), *AtIRX3* for xylem (19), and *AtML1* for epidermis (20). These promoter cassettes drive reporter GUS activity in the corresponding tissue layers in the inflorescence stems (Fig. S1 *A–C*). Expression of the *ER-FLAG* transgenes was confirmed by RT-PCR (Fig. S1 *D–F*). *er* plants exhibit characteristic compact inflorescences with flowers cluster-

Author contributions: N.U., J.S.L., M.T., and K.U.T. designed research; N.U., J.S.L., H.-H.L., and K.U.T. performed research; N.U., J.S.L., R.K., T.K., and K.U.T. contributed new reagents/analytic tools; N.U., J.S.L., R.J.H., and K.U.T. analyzed data; and N.U., J.S.L., R.J.H., and K.U.T. wrote the paper.

The authors declare no conflict of interest.

This article is a PNAS Direct Submission.

Freely available online through the PNAS open access option.

Data deposition: The data reported in this paper have been deposited in the Gene Expression Omnibus (GEO) database, www.ncbi.nlm.nih.gov/geo (accession no. GSE35166).

[1]N.U. and J.S.L. contributed equally to this work.

[2]To whom correspondence should be addressed. E-mail: ktorii@u.washington.edu.

This article contains supporting information online at www.pnas.org/lookup/suppl/doi:10.1073/pnas.1117537109/-/DCSupplemental.

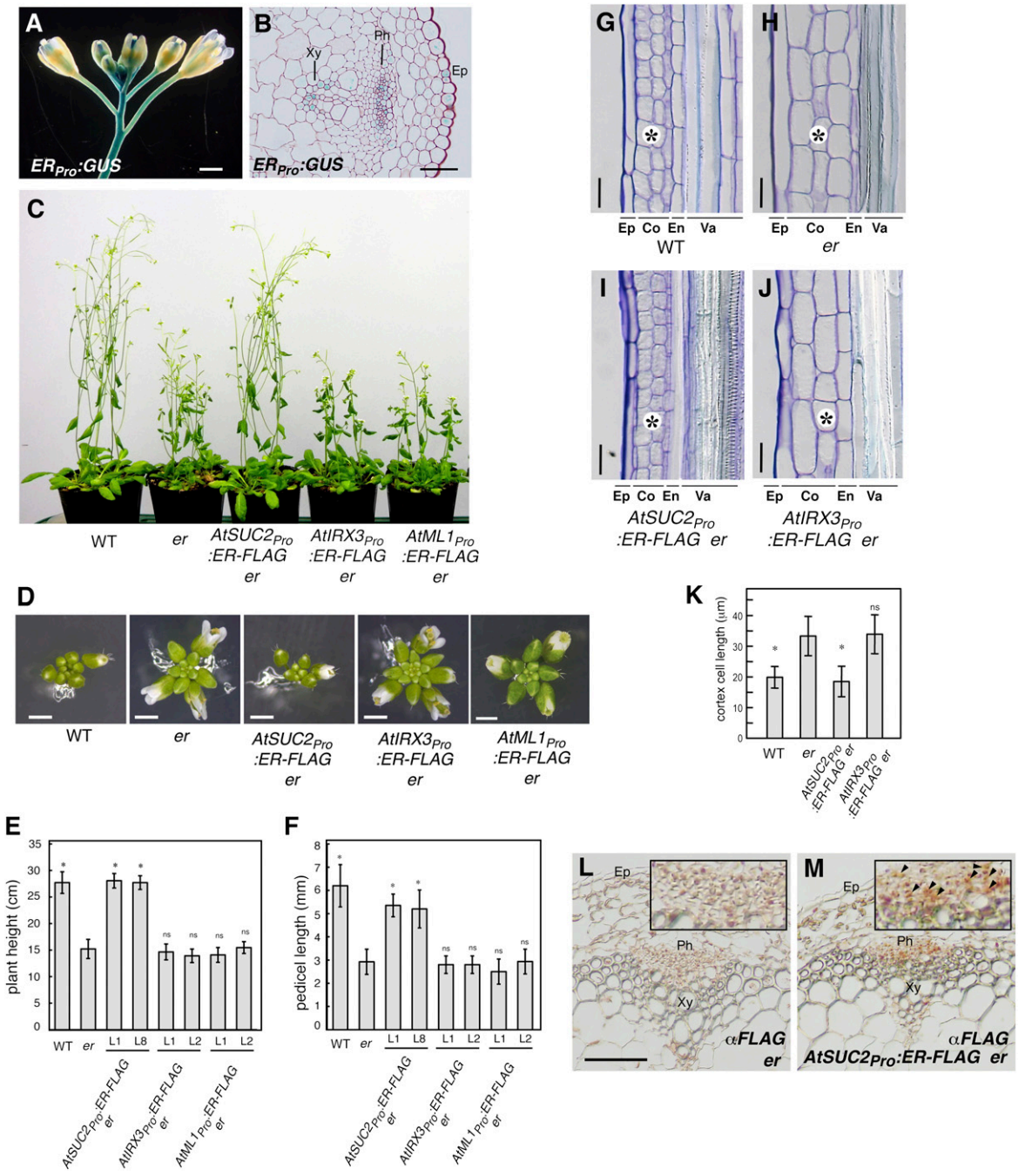

Fig. 1. Phloem-specific expression of *ER* is sufficient to restore normal inflorescence architecture of *er*. (*A* and *B*) *ERpro:GUS* expression pattern in inflorescence (*A*) and stem cross- section (*B*). Ep, epidermis; Ph, phloem; Xy, xylem. (Scale bars: 1 mm in *A*; 50 μm in *B*.) (*C*) Five-wk-old plants of WT, *er*, and *er*-expressing *AtSUC2pro:ER-FLAG*, *AtIRX3pro:ER-FLAG*, and *AtML1pro:ER-FLAG*. (*D*) Top view of representative inflorescence from respective genotypes. (Scale bars: 1 mm.) (*E* and *F*) Morphometric analysis of plant height (*E*) and pedicel length (*F*) from each genotype. Five-wk-old plants ($n = 7$) were measured for plant height, and 6-wk-old mature pedicels ($n = 20$, from 5 plants; $n = 14$ for *AtML1pro:ER-FLAG* line 2) were measured. Bars indicate mean values; error bars indicate SD. *Significantly different from *er* ($P < 0.0001$, Student *t* test), but not from WT [Tukey's honestly significant difference (HSD) test]; ns, not significantly different from *er*. (*G–J*) Longitudinal sections of mature pedicels. Ep, epidermis; Co, cortex; En, endodermis; Va, vasculature. (Scale bar: 25 μm.) (*K*) Quantitative analysis of cortex cell length ($n = 26–30$). Bars indicate mean values; error bars indicate SD. *Significantly different from *er* ($P < 0.0001$, Student *t* test); ns, not significant from *er*. (*L* and *M*) Immunohistochemical analysis of inflorescence stem sections of er (*L*) and *AtSUC2pro:ER-FLAG er* (*M*) using anti-FLAG antibody. Strong orange-brown signals are detected in the phloem (Ph) tissues in *AtSUC2pro:ER-FLAG* (*M*, *Inset*; arrowheads).

ing at the top (5). *AtML1pro:ER-FLAG* and *AtIRX3pro:ER-FLAG* conferred no phenotypic effects on the inflorescence in *er* (Fig. 1 *C–F*). In contrast, *AtSUC2pro:ER-FLAG er* inflorescence phenotypes were indistinguishable from that of WT plants (Fig. 1 *C–F*). In addition, *AtSUC2pro:ER-FLAG* rescued leaf and silique elongation defects of *er* (Fig. S2).

er stems and pedicels are known to have reduced cell proliferation, notably in the cortex, accompanied by compensatory cell growth (17, 21). We further examined the underlying cellular basis of phenotypic rescue by *AtSUC2pro:ER-FLAG*. Cortex cells in *AtSUC2pro:ER-FLAG er* pedicels were indistinguishable from WT: small, rectangular, and organized (Fig. 1 *G*, *I*, and *K*). In

contrast, cortex cells in *er* pedicels expressing *AtIRX3pro:ER-FLAG*, which failed to complement the *er* aboveground phenotype, were indistinguishable from *er* (Fig. 1 *H*, *J*, and *K*).

Because ER is a transmembrane protein (5, 22), its movement from the phloem to the cortex tissues to control cell proliferation is highly unlikely. To examine this, we performed an immunohistochemical analysis of *AtSUC2pro:ER-FLAG er* inflorescence stems using anti-FLAG antibody (Fig. 1 *L* and *M*). AtSUC2::ER-FLAG protein was detected only in the phloem tissues (Fig. 1*M*). Taken together, our findings indicate that phloem-specific expression of *ER* is sufficient for proper inflorescence architecture and imply that *ER* coordinates cell proliferation in the inflorescence in a non–cell-autonomous manner.

Secreted Peptide Genes *EPFL4* and *EPFL6/CHAL* Control Inflorescence Growth in the *ER* Pathway. To identify signaling ligands for ER in phloem-mediated inflorescence growth, we surveyed the *EPFL* family genes that we identified in a previous study (9). EPF1 and EPF2, two founding members of the family, suppress stomatal differentiation as upstream signals for ER family RLKs (8, 9). We previously found that overexpression of *EPFL4* or *EPFL5* also suppresses stomatal differentiation (9), implying that these genes can act as ligands for ER family members in the epidermis when ectopically expressed. Molecular phylogeny has shown that *EPFL4* and *EPFL5* are recently duplicated paralogs most closely related to *EPFL6/CHAL*, which influences *TMM*-mediated stomatal patterning in hypocotyls (14) (Fig. 2*A*). Based on this evidence, we prioritized our analysis on the *EPFL4/5/6* subfamily.

Similar to *ERpro:GUS* (Fig. 1*A*), both *EPFL4pro:GUS* and *EPFL6pro:GUS* show strong staining in inflorescence stems (Fig. 2*B*), suggesting that they are likely candidates. In contrast, *EPFL5pro:GUS* exhibited activity in developing flowers, but not in inflorescence stems (Fig. 2*B*).

We next investigated the loss-of-function phenotypes of *EPFL4/5/6*. The T-DNA insertion alleles of *EPFL4* and *EPFL6* do not accumulate detectable transcripts (Fig. S3), indicating that they are null. The available *epfl5* T-DNA lines appear to knock down expression (Fig. S3). Although *epfl4* or *epfl6/chal-2* single mutants exhibited no detectable inflorescence phenotypes, *epfl4 epfl6/chal-2* double-mutant plants developed a compact inflorescence with clustered flowers, a phenotype identical to *er* (Fig. 2*C*). Furthermore, tissue sectioning of *epfl4 epfl6/chal-2* pedicels revealed large and expanded cortex cells resembling (and not significantly different from) that of *er* (Fig. 2 *F–J*), indicating that *epfl4 epfl6/chal-2* and *er* have the same underlying cellular defects. Morphometric analysis places the phenotypic severity of *epfl4 epfl6/chal-2* between the null allele *er-105* and the intermediate allele *er-103* (Fig. 2 *D* and *E*). Additional introduction of *epfl5* (*epfl4 epfl5 epfl6/chal-2* triple) did not affect inflorescence architecture, but did confer fruit sterility (Fig. S3*D*), consistent with the absence of *EPFL5* promoter activity in

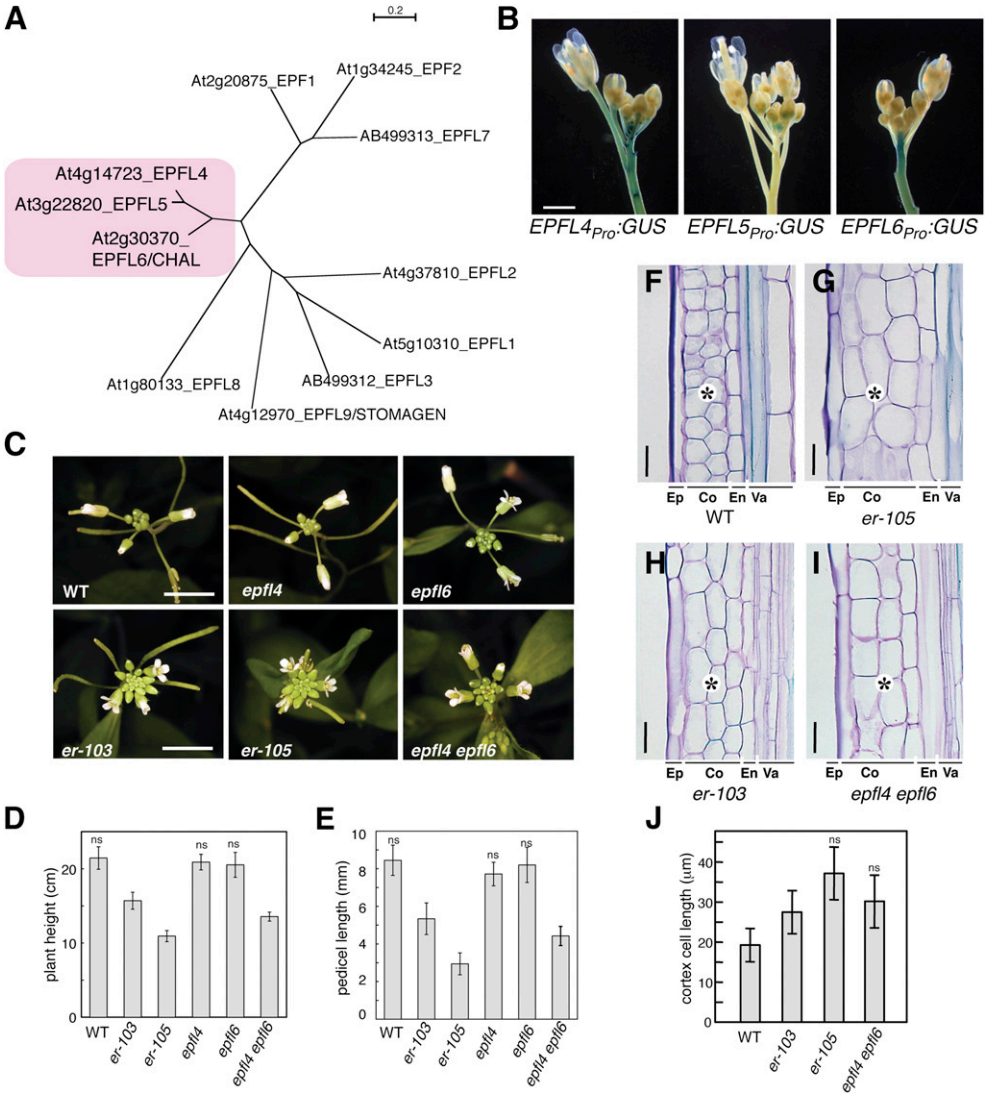

Fig. 2. *EPFL4* and *EPFL6* redundantly control inflorescence growth in a manner similar to *ER*. (*A*) Molecular phylogeny of EPFL family members. *EPFL4*, *EPFL5*, and *EPFL6* cluster together. Shown is an unrooted neighbor-joining tree of C-terminal end amino acid sequence encompassing the predicted mature EPF (MEPF) domain. Branch lengths are scaled to the number of amino acid changes indicated on the scale bar. MEPF sequence alignment is shown in Fig. S8. (*B*) Promoter activities of *EPFL4*, *EPFL5*, and *EPFL6* in inflorescence. (Scale bar: 1 mm.) (*C*) *epfl4 epfl6/chal-2* confers compact inflorescence nearly identical to that of *er*. Shown are inflorescence tops of 5-wk-old *Arabidopsis* of WT, *epfl4*, *epfl6*, *er-103* (intermediate allele), *er-105* (null allele), and *epfl4 epfl6/chal-2*. (Scale bars: 1 cm.) (*D* and *E*) Morphometric analysis of plant height (D) and pedicel length (*E*) from each genotype. 5-wk-old plants were measured for plant height (n = 9), and 6-wk-old mature pedicels (n = 46, from 6 plants) were measured. Bars indicate mean values; error bars indicate SD. ns, not significantly different and grouped together (Tukey's HSD test). (*F–I*) Longitudinal sections of mature pedicels from WT (*F*), *er-105* (*G*), *er-103* (*H*), and *epfl4 epfl6/chal-2* (*I*). Ep, epidermis; Co, cortex; En, endodermis; Va, vasculature. *epfl4 epfl6* has large cortex cells similar to *er* (asterisks). (Scale bars: 25 μm.) (*J*) Quantitative analysis of cortex cell length (n = 30). Bars indicate mean values; error bars indicate SD. ns, not significantly different and grouped together (Tukey's HSD test). The images in each composite were obtained under the same magnification.

inflorescence stems (Fig. 2*B*). Despite the strong resemblance of *epfl4 epfl6*/*chal-2* and *er*, stomatal patterning in *epfl4 epfl6*/*chal-2* cotyledon and stem epidermis was normal, suggesting that these mutants normally have no effect on stomatal development (Fig. S4).

To determine whether *EPFL4* and *EPFL6* act in the *ER* pathway, we tested whether the ectopic overexpression phenotypes of *EPFL4* and *EPFL6* in the epidermis are ER-dependent. *CaMV35Spro:EPFL4* and *CaMV35Spro:EPFL6* inhibited stomatal differentiation in WT backgrounds. These ectopic effects were diminished in *er* (Fig. S5). Taken together, these findings suggest that EPFL4 and EPFL6 redundantly promote inflorescence growth in the ER pathway.

Endodermal Expression of *EPFL4* or *EPFL6* Is Sufficient for Proper Inflorescence Architecture. From which tissue layer are EPFL4 and EPFL6 signals generated to promote inflorescence growth? Tissue sectioning shows that both *EPFL4pro:GUS* and *EPFL6-pro:GUS* are active predominantly within the endodermis of inflorescence stems (Fig. 3 *A*–*D*). To address whether the endodermis is necessary for the observed expression of *EPFL4* and *EPFL6*, the GUS reporters were crossed into *short-root* (*shr*) mutant (also known as *sgr7*), which fails to differentiate endodermis in roots and shoots (2, 23). Drastic reduction in GUS activity was observed in *shr* (Fig. 3 *E* and *F*), further supporting the finding that *EPFL4* and *EPFL6* promoters are active predominantly within the endodermis. *EPFL4pro:GUS* also stained the base of pedicels, apparently independent of the endodermal expression (Fig. 3*E*).

To investigate whether the endodermal expression of *EPFL4* or *EPFL6* is sufficient to rescue the *er*-like inflorescence phenotype of *epfl4 epfl6*, we expressed *EPFL4* and *EPFL6* under the *SCARECROW* (*SCR*) promoter, which drives endodermal expression in both roots and shoots (24) (Fig. 3 *G*–*L*). The *epfl4 epfl6* plants expressing *SCRpro:EPFL4* and *SCRpro:EPFL6* exhibited an elongated inflorescence with flower buds completely covering the SAM, a phenotype indistinguishable from that of WT (Fig. 3 *G*–*J*). Morphometric and statistical analyses further supported that *SCRpro:EPFL4* and *SCRpro:EPFL6* fully restore both plant height and pedicel length to the levels in WT (Fig. 3 *K* and *L*). We conclude that *EPFL4* and *EPFL6* are expressed predominantly in inflorescence endodermis, and that their endodermal expression is sufficient for the proper development of inflorescence architecture.

EPFL4 and EPFL6 Associate with ER in Planta. Our genetic studies suggest that EPFL4 and EPFL6 peptide signals originate from the endodermis and are perceived by the cell-surface receptor ER in the neighboring phloem tissue. We examined whether EPFL4 and EPFL6 associate with ER through coimmunoprecipitation (co-IP) experiments (Fig. 4). Epitope-tagged EPFL4 and EPFL6 were expressed in the presence or absence of an epitope-tagged ER in *Nicotiana benthamiana*. The *EPFL* genes belong to a superfamily of

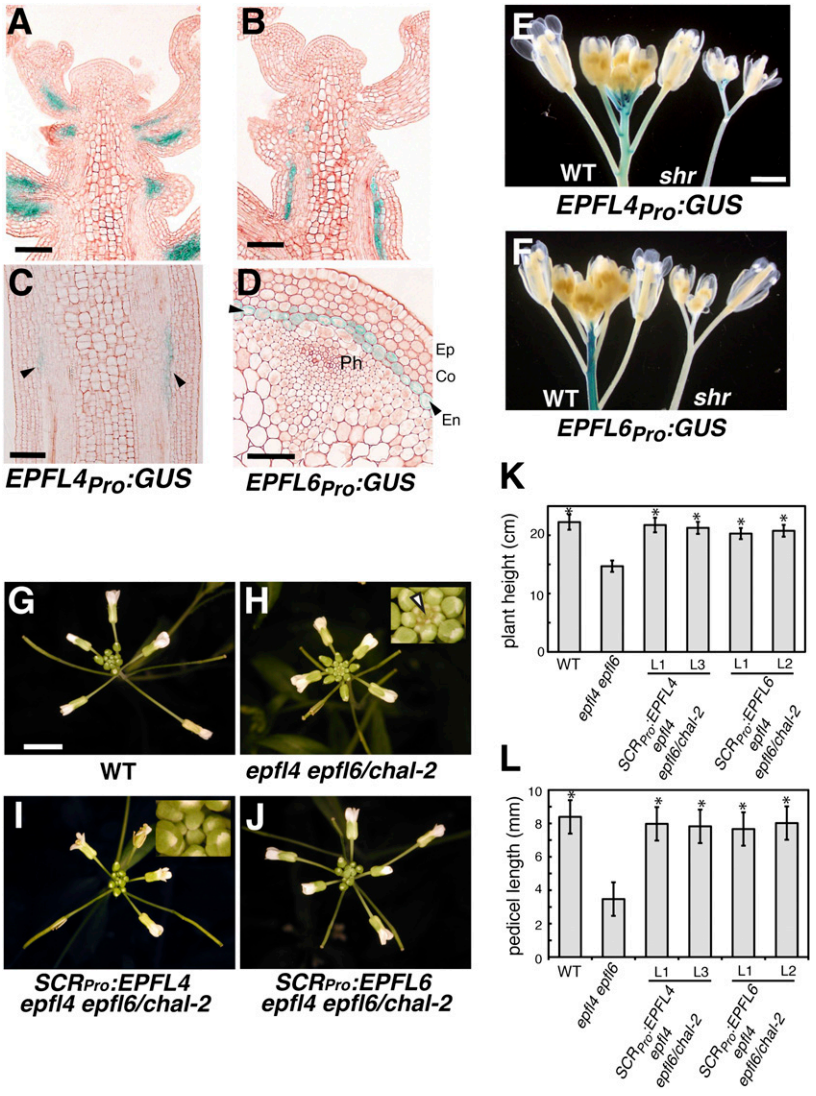

Fig. 3. Endodermis-specific expression of *EPFL4* or *EPFL6* is sufficient to restore normal inflorescence architecture of *epfl4 epfl6*. (*A*–*D*) *EPFL4* and *EPFL6* promoters are predominantly active in the endodermis of inflorescence stems and pedicels. Shown are longitudinal sections of inflorescence tips expressing *EPFL4pro:GUS* (*A*) or *EPFL6-pro:GUS* (*B*) and their stem sections at higher magnifications in longitudinal sections (*C*) or cross-sections (*D*). Arrowheads indicate endodermal GUS expression. Ep, epidermis; Co, cortex; En, endodermis; Ph, phloem. (Scale bars: 20 μm in *A* and *B*, 10 μm in *C* and *D*.) (*E* and *F*) GUS activities of *EPFL4pro:GUS* (*E*) and *EPFL6pro:GUS* (*F*) are severely reduced in *shr* mutant lacking endodermis. (*G*–*J*) Expression of *EPFL4* and *EPFL6* driven by the endodermis-specific *SCR* promoter fully rescues the inflorescence growth phenotype of *epfl4 epfl6*. Shown are top views of 4-wk-old inflorescence from WT (*G*), *epfl4 epfl6*/*chal-2* (*H*), *SCRpro:EPFL4* in *epfl4 epfl6*/*chal-2* (*I*), and *SCRpro:EPFL6* in *epfl4 epfl6*/*chal-2* (*J*). (*Insets*) *epfl4 epfl6*/*chal-2* exhibits characteristic flat inflorescence top with exposed SAM (*H*; arrowhead), while in rescued plants flower buds cover SAM (*I*). (Scale bar: 5 mm.) (*K* and *L*) Morphometric analysis showing heights of 5-wk-old plants (n = 7–8) and lengths of mature pedicels (n = 63) from 6-wk-old plants of each genotype. Bars indicate mean values; error bars indicate SD. *Significantly different from *epfl4 epfl6*/*chal-2* (P < 0.0001, Student t test), but not from WT.

CRPs (25). As a control, we expressed LURE2, an unrelated CRP from *Torenia fournieri* involved in pollen tube guidance (26). Co-IP experiments showed that EPFL4-FLAG and EPFL6-FLAG associate with ERΔK-GFP (22) (Fig. 4). In contrast, LURE2-FLAG did not associate with ERΔK-GFP despite its abundant expression (Fig. 4). These results demonstrate that EPFL4 and EPFL6 specifically associate with ER in planta.

Transcriptome Analysis Reveals Potential Mechanisms of Inflorescence Growth Mediated by EPFL4/6-ER Ligand–Receptor Pathway. To gain insight into the mechanisms of inflorescence development mediated by the EPFL4/6-ER signaling module, we examined global inflorescence transcriptomes of WT, *er*, and *epfl4 epfl6/chal-2*. Among commonly up-regulated or down-regulated genes (57 and 42, respectively: Fig. S6*A*) in *er* and *epfl4 epfl6,* a significant overrepresentation was found in the categories "hormone metabolism" and "signaling" (Dataset S1). Of note, auxin-regulated genes and GA metabolic genes were among the differentially regulated genes (DRGs) (Fig. S6*B*), including down-regulation of auxin-induced *ARGOS* (threefold in both *er* and *epfl4 epfl6/chal-2*), which promotes aboveground organ growth (27).

The commonly down-regulated genes may represent downstream targets of the EPFL4/6-ER signaling module. Among the transcription factor (TF) genes, *WRKY15* was significantly down-regulated (by threefold) in both *er* and *epfl4 epfl6/chal-2* (Fig. S6*B*). Consistently, W-box motifs, binding sites for WRKY-family TFs, were significantly ($P < 0.001$) enriched in the promoters of commonly down-regulated genes, suggesting a possible role of WRKY TFs downstream of ER. Although delineating specific relationships of these DRGs to EPFL4/6 ER-mediated inflorescence growth needs further study, our results suggest the potential roles for plant hormones in ER-mediated non–cell-autonomous control of inflorescence architecture.

Discussion

Here we present genetic and biochemical evidence indicating that ER perceives two EPFL peptides, EPFL4 and EPFL6, to promote inflorescence growth. Our finding suggests that cell–cell communication between the endodermis and phloem, mediated by peptide ligands and a receptor kinase, plays an important role in coordinated growth of *Arabidopsis* inflorescence (Fig. S7*A*).

In sharp contrast to their *er*-like inflorescence architecture, *epfl4 epfl6/chal-2* plants do not exhibit stomatal patterning defects, and these genes are not expressed in the epidermis (Fig. 3 and Fig. S4). Thus, these two EPFLs act primarily as positive regulators of inflorescence growth, not in stomatal patterning under normal conditions. *chal* has been identified as a suppressor of *tmm*, partially restoring stomatal differentiation in *tmm* hypocotyls (14). Given that *ER* family genes become overly inhibitory for stomatal differentiation in *tmm* hypocotyls and stems (7), it is conceivable that a small bleed-through of EPFL6 signals from the endodermis influences ER family activity in the epidermis as a secondary consequence of missing TMM. While this paper was in preparation, Abrash et al. (15) reported that additional losses of function in *EPFL4/CHAL-LIKE2* (*CLL2*) and *EPFL5/CLL1* further diminish the effects of *tmm*, and proposed that TMM generates signaling specificity for the ER family within the epidermis. Intertissue layer ligand–receptor interaction also occurs within the vasculature, where the CLE peptide TDIF secreted from the phloem is perceived by an LRR-RLK, PXY/TDR, expressed in the adjacent procambium to enforce vascular division polarity (28, 29). It would be interesting to know whether a signal modulator like TMM exists in the internal tissues for ER family and other receptors, such as PXY/TDR, to enhance signaling specificity.

Although three *ER* family genes, *ER*, *ERL1*, and *ERL2*, are known to synergistically promote aboveground organ morphogenesis (17), introduction of the phloem-expressed *ER* fully rescued the inflorescence phenotype of *er erl1 erl2* (Fig. S7*B*). This clearly indicates that ERLs play a negligible role in EPFL4/6-mediated inflorescence elongation. The severe dwarfism and floral growth defects in *er erl1 erl2* triple-mutant plants (17) might be related to the additional roles of ERLs in the SAM structure and function, which may require yet another *EPFL* member. Consistent with this idea, *EPFL5*, which is not expressed in the stem endodermis, promotes fruit growth and fertility (Fig. S3) in a manner similar to higher-order mutants in the *ER* family (30).

Our transcriptome analysis revealed overrepresentation of auxin and GA-related genes among DRGs (Fig. S6 and Dataset S1), implying that inflorescence growth via EPFL4/6-ER signaling ultimately involves these two hormones, which act non–cell-autonomously to promote cortex cell proliferation. The ER-signaling pathway consistently interacts genetically with these two hormones (31–33). Alternatively, deregulation of auxin/GA genes in *er* and *epfl4 epfl6/chal-2* might be a secondary consequence of having compact inflorescence. Further dissection of the EPFL4/6-ER signaling module will clarify these possibilities.

Among the commonly down-regulated DRGs, W-box sites are overrepresented and *WRKY15* is down-regulated in *epfl4 epfl6* and *er* (Fig. S6). WRKY15 is one of the five TFs predicted to be downstream of ER-signaling based on a bioinformatics study that combined seedling expression quantitative trait loci data from L*er*/Cvi recombinant inbred lines and L*er* microarray data (34). We propose that ER represents a major receptor for at least two distinct signaling pathways, the EPF1/2-mediated pathway inhibiting stomatal development via targeting bHLH TFs (35, 36) and the EPFL4/6-mediated pathway promoting aboveground organ growth, where WRKY15 may act downstream. Our findings provide insight into how a broadly expressed RLK mediates distinct developmental responses in plants.

Interactions between the epidermis and inner tissue have been the major focus in studies examining how different tissue layers contribute to aboveground organ growth and development (37, 38). For instance, epidermis-specific expression of brassinosteroid receptor BRI1 was found to fully rescue the dwarf inflorescence phenotype of *bri1* (37). Unlike *BRI1*, *ER* driven by the same *AtML1* promoter used in the foregoing study does not rescue inflorescence growth (Fig. 1 *D*–*F*). Our work illuminates a previously unanticipated role for the endodermis and phloem in growth coordination and the presence of multiple layers of cell–cell signaling across tissue layers that promote plant aboveground development.

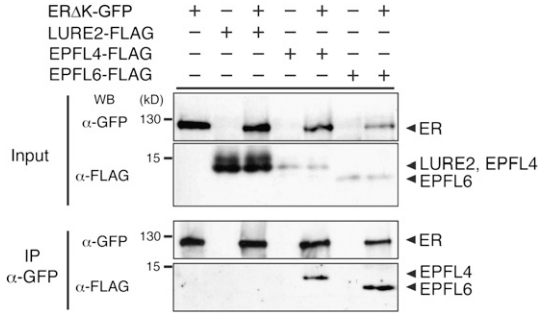

Fig. 4. EPFL4 and EPFL6 associate with ER in planta. Shown are co-IP assays of epitope-tagged ligand–receptor pairs expressed in *N. benthamiana* leaves. ER associates with EPFL4-FLAG and EPFL6-FLAG but not with a control, LURE2-FLAG. The faint, higher molecular bands in ligand inputs likely represent unprocessed/intermediate precursors. Molecular mass is expressed in kilodaltons. All experiments were repeated at least four times.

Materials and Methods

Plant Materials. The *Arabidopsis* ecotype Columbia (Col) was used as WT. *er-2* (CS3401), *epfl4* (Salk_071065), *epfl5* (Salk_005080), and *epfl6/chal-2* (Salk_072522) were obtained from the *Arabidopsis* Biological Resource Center. *epfl4*, *epfl5*, and *epfl6/chal-2* were backcrossed to WT Col three times before characterization. PCR-based genotyping was performed using the primer pairs listed in Dataset S1. Double mutants were generated by genetic crosses. The following materials were reported previously: *er-103*, *er-105* (5), and *sgr7-1/shr* (2). Seedlings and plants were grown as described previously (39).

Molecular Cloning and Generation of Transgenic Plants. Dataset S1 lists the plasmid constructs generated in this study along with the primer DNA sequences used for molecular cloning. A functional *ER* coding sequence

containing introns (40) was used for epitope-tagged constructs. *Agrobacterium tumefaciens* strain GV3101 was used for plant transformation via the floral dip method. More than 15 T1 plants were selected for each construct, and at least two lines were selected for each construct based on single-insertion status inferred by the segregation of resistance genes and stability of the phenotype in subsequent generations. *AtSUC2pro:ER-FLAG* and *AtIRX3pro:ER-FLAG* were transformed into *er-2*, and *AtML1pro:ER-FLAG* was transformed into *er-105*.

Histological Analysis and Microscopy. GUS staining was done as described previously (41). To make plastic sections, samples were fixed in formalin/acetic acid/alcohol and embedded in Technovit 7100 resin (Heraeus Kulzer, Wehrheim, Germany). Then 4-μm sections were prepared and stained with 0.02% toluidine blue or 0.04% neutral red. The cortex cell length was measured using Adobe Photoshop CS3. Confocal microscopy was performed as described previously (39). Immunohistochemistry was performed using paraformaldehyde-fixed materials as described previously (41) but using the Vectastain Elite ABC Mouse IgG Kit (Vector Laboratories) instead of ImmPRESS reagent Anti-Mouse IgG (Vector Laboratories).

RT-PCR. RNA extraction, cDNA synthesis, and RT-PCR were performed as described previously (39). Primer sequences are listed in Dataset S1.

Transient Protein Expression, Co-IP, and Protein Gel Blot Immunoanalysis. *A. tumefaciens* strain GV3101 was transformed with expression clones and grown in yeast extract and beef medium supplemented with relevant antibiotics. Bacterial cultures were precipitated and resuspended in infiltration medium [10 mM $MgCl_2$, 10 mM MES (pH 5.6), and 150 μM acetosyringone]. To enhance transient expression in tobacco, the silencing suppressor p19 was coinfiltrated (42). The bacterial suspensions were infiltrated into young but fully expanded leaves of *N. benthamiana* plants using a 1-mL syringe barrel. After infiltration, plants were cultivated at 25 °C and collected for further biochemical assays after 48–72 h. Protein extraction, co-IP using anti-GFP antibody (ab290; Abcam), and protein gel immunoblot analysis using anti-GFP (Invitrogen) and anti-FLAG M2 (Sigma-Aldrich) antibodies were performed as described previously (22).

Microarray and Statistical Analysis. Developing inflorescence tips from 33-d-old WT Col, *er-2*, and *epfl4 epfl6/chal-2* were subjected to RNA preparation, cDNA synthesis, and hybridization to Affymetrix ATH1 chips. *er-2* was used because *er-105* carries an additional *gl1* mutation (5). Three biological replicates were used. The protocol and bioinformatics analyses are described in more detail in *SI Materials and Methods*.

ACKNOWLEDGMENTS. We thank A. Rychel for molecular phylogenetic analysis; J. Dahl, J. Sagawa, B. Burrows, and A. Cloutier for assistance; the *Arabidopsis* Biological Resource Center and the Salk Institute Genome Analysis Laboratory for T-DNA insertion lines; D. Baulcombe for p19; M. Kanaoka and M. T. Morita for plasmids; S. Betsuyaku for Agroinfiltration protocols; and L. Pillitteri, K. Peterson, and M. Kanaoka for commenting on the manuscript. This work was supported by National Science Foundation Grant IOS-0744892 (to K.U.T.); the Japan Science and Technology Agency [a Precursory Research for Embryonic Science and Technology (PRESTO) award (to K.U.T.)]; Japanese Ministry of Education, Culture, Sports, Science, and Technology Grants-in-Aid for Scientific Research B 22370019, Priority Areas 19060007, and Exploratory Research 22657015 (to M.T.), and Grants-in-Aid for Young Scientists B 20770035 and 22770038 (to N.U.); and the Sumitomo Foundation (N.U.). J.S.L. is a Natural Sciences and Engineering Research Council of Canada postdoctoral fellow, R.J.H. is a Deutsche Forschungsgemeinschaft postdoctoral fellow, H.-H.L. is an American Society of Plant Biologists summer undergraduate research fellow, and K.U.T. is a Howard Hughes Medical Institute–Gordon and Betty Moore Foundation investigator.

1. Javelle M, Vernoud V, Rogowsky PM, Ingram GC (2011) Epidermis: The formation and functions of a fundamental plant tissue. *New Phytol* 189:17–39.
2. Fukaki H, et al. (1998) Genetic evidence that the endodermis is essential for shoot gravitropism in *Arabidopsis thaliana*. *Plant J* 14:425–430.
3. Turner S, Sieburth LE (2003) Vascular patterning. *Arabidopsis Book* 2:e0073.
4. Rédei GP (1962) Single-locus heterosis. *Z Vererbungsl* 93:164–170.
5. Torii KU, et al. (1996) The *Arabidopsis ERECTA* gene encodes a putative receptor protein kinase with extracellular leucine-rich repeats. *Plant Cell* 8:735–746.
6. van Zanten M, Snoek LB, Proveniers MC, Peeters AJ (2009) The many functions of ERECTA. *Trends Plant Sci* 14:214–218.
7. Shpak ED, McAbee JM, Pillitteri LJ, Torii KU (2005) Stomatal patterning and differentiation by synergistic interactions of receptor kinases. *Science* 309:290–293.
8. Hara K, Kajita R, Torii KU, Bergmann DC, Kakimoto T (2007) The secretory peptide gene *EPF1* enforces the stomatal one-cell -spacing rule. *Genes Dev* 21:1720–1725.
9. Hara K, et al. (2009) Epidermal cell density is autoregulated via a secretory peptide, EPIDERMAL PATTERNING FACTOR 2, in *Arabidopsis* leaves. *Plant Cell Physiol* 50:1019–1031.
10. Hunt L, Gray JE (2009) The signaling peptide EPF2 controls asymmetric cell divisions during stomatal development. *Curr Biol* 19:864–869.
11. Nadeau JA, Sack FD (2002) Control of stomatal distribution on the *Arabidopsis* leaf surface. *Science* 296:1697–1700.
12. Kondo T, et al. (2010) Stomatal density is controlled by a mesophyll-derived signaling molecule. *Plant Cell Physiol* 51:1–8.
13. Sugano SS, et al. (2010) Stomagen positively regulates stomatal density in *Arabidopsis*. *Nature* 463:241–244.
14. Abrash EB, Bergmann DC (2010) Regional specification of stomatal production by the putative ligand CHALLAH. *Development* 137:447–455.
15. Abrash EB, Davies KA, Bergmann DC (2011) Generation of signaling specificity in *Arabidopsis* by spatially restricted buffering of ligand–receptor interactions. *Plant Cell* 23:2864–2879.
16. Yokoyama R, Takahashi T, Kato A, Torii KU, Komeda Y (1998) The *Arabidopsis ERECTA* gene is expressed in the shoot apical meristem and organ primordia. *Plant J* 15:301–310.
17. Shpak ED, Berthiaume CT, Hill EJ, Torii KU (2004) Synergistic interaction of three ERECTA family receptor-like kinases controls *Arabidopsis* organ growth and flower development by promoting cell proliferation. *Development* 131:1491–1501.
18. Imlau A, Truernit E, Sauer N (1999) Cell-to-cell and long-distance trafficking of the green fluorescent protein in the phloem and symplastic unloading of the protein into sink tissues. *Plant Cell* 11:309–322.
19. Gardiner JC, Taylor NG, Turner SR (2003) Control of cellulose synthase complex localization in developing xylem. *Plant Cell* 15:1740–1748.
20. Sessions A, Weigel D, Yanofsky MF (1999) The *Arabidopsis thaliana MERISTEM LAYER 1* promoter specifies epidermal expression in meristems and young primordia. *Plant J* 20:259–263.
21. Shpak ED, Lakeman MB, Torii KU (2003) Dominant-negative receptor uncovers redundancy in the *Arabidopsis* ERECTA leucine-rich repeat receptor-like kinase signaling pathway that regulates organ shape. *Plant Cell* 15:1095–1110.
22. Lee JS, et al. (2012) Direct interaction of ligand–receptor pairs specifying stomatal patterning. *Genes Dev* 26:126–136.
23. Helariutta Y, et al. (2000) The *SHORT-ROOT* gene controls radial patterning of the *Arabidopsis* root through radial signaling. *Cell* 101:555–567.
24. Wysocka-Diller JW, Helariutta Y, Fukaki H, Malamy JE, Benfey PN (2000) Molecular analysis of *SCARECROW* function reveals a radial patterning mechanism common to root and shoot. *Development* 127:595–603.
25. Higashiyama T (2010) Peptide signaling in pollen–pistil interactions. *Plant Cell Physiol* 51:177–189.
26. Okuda S, et al. (2009) Defensin-like polypeptide LUREs are pollen tube attractants secreted from synergid cells. *Nature* 458:357–361.
27. Hu Y, Xie Q, Chua NH (2003) The *Arabidopsis* auxin-inducible gene *ARGOS* controls lateral organ size. *Plant Cell* 15:1951–1961.
28. Fisher K, Turner S (2007) PXY, a receptor-like kinase essential for maintaining polarity during plant vascular tissue development. *Curr Biol* 17:1061–1066.
29. Hirakawa Y, et al. (2008) Non–cell-autonomous control of vascular stem cell fate by a CLE peptide/receptor system. *Proc Natl Acad Sci USA* 105:15208–15213.
30. Pillitteri LJ, Bemis SM, Shpak ED, Torii KU (2007) Haploinsufficiency after successive loss of signaling reveals a role for ERECTA-family genes in *Arabidopsis* ovule development. *Development* 134:3099–3109.
31. Fridborg I, Kuusk S, Moritz T, Sundberg E (1999) The *Arabidopsis* dwarf mutant *shi* exhibits reduced gibberellin responses conferred by overexpression of a new putative zinc finger protein. *Plant Cell* 11:1019–1032.
32. Kanyuka K, et al. (2003) Mutations in the huge *Arabidopsis* gene *BIG* affect a range of hormone and light responses. *Plant J* 35:57–70.
33. Woodward C, et al. (2005) Interaction of auxin and ERECTA in elaborating *Arabidopsis* inflorescence architecture revealed by the activation tagging of a new member of the YUCCA family of putative flavin monooxygenases. *Plant Physiol* 139:192–203.
34. Terpstra IR, Snoek LB, Keurentjes JJ, Peeters AJ, van den Ackerveken G (2010) Regulatory network identification by genetical genomics: Signaling downstream of the *Arabidopsis* receptor-like kinase ERECTA. *Plant Physiol* 154:1067–1078.
35. Peterson KM, Rychel AL, Torii KU (2010) Out of the mouths of plants: The molecular basis of the evolution and diversity of stomatal development. *Plant Cell* 22:296–306.
36. Rowe MH, Bergmann DC (2010) Complex signals for simple cells: The expanding ranks of signals and receptors guiding stomatal development. *Curr Opin Plant Biol* 13:548–555.
37. Savaldi-Goldstein S, Peto C, Chory J (2007) The epidermis both drives and restricts plant shoot growth. *Nature* 446:199–202.
38. Savaldi-Goldstein S, Chory J (2008) Growth coordination and the shoot epidermis. *Curr Opin Plant Biol* 11:42–48.
39. Pillitteri LJ, Peterson KM, Horst RJ, Torii KU (2011) Molecular profiling of stomatal meristemoids reveals new component of asymmetric cell division and commonalities among stem cell populations in *Arabidopsis*. *Plant Cell* 23:3260–3275.
40. Karve R, Liu W, Willet SG, Torii KU, Shpak ED (2011) The presence of multiple introns is essential for *ERECTA* expression in *Arabidopsis*. *RNA* 17:1907–1921.
41. Uchida N, Igari K, Bogenschutz NL, Torii KU, Tasaka M (2011) *Arabidopsis* ERECTA-family receptor kinases mediate morphological alterations stimulated by activation of NB-LRR type UNI proteins. *Plant Cell Physiol* 52:804–814.
42. Voinnet O, Rivas S, Mestre P, Baulcombe D (2003) An enhanced transient expression system in plants based on suppression of gene silencing by the p19 protein of tomato bushy stunt virus. *Plant J* 33:949–956.